# Reproducible chemostat cultures to eliminate eukaryotic viruses from fecal transplant material

Signe Adamberg[1], Torben Sølbeck Rasmussen[2], Sabina Brigitte Larsen[2], Xiaotian Mao[1], Dennis Sandris Nielsen[2], Kaarel Adamberg[1,3]

[1]Department of Chemistry and Biotechnology, Tallinn University of Technology, Akadeemia tee 15, Tallinn, Estonia

[2]Section of Microbiology and Fermentation, Department of Food Science, University of Copenhagen

[3]Center of Food and Fermentation Technologies, Mäealuse 2/4, 12618, Tallinn, Estonia

## ABSTRACT

The effect of fecal microbiota transplantation (FMT) on various gut-related diseases is intensively investigated in clinical trials. In addition to bacteria, the gut microbiome also contains eukaryotic, archaeal, and bacterial viruses (bacteriophages, in short phages), which collectively is referred to as the gut virome. Application of FMT in clinical settings is associated with a potential risk for the recipient of transferring infectious eukaryotic viruses or bacteria, despite strict screening procedures for the donor material. A safer and more targeted method to modulate the gut microbiota is therefore needed to extend the application width of FMT. Emerging evidence suggests that gut phages play a key role in maintaining a balanced gut microbiome as well as in FMT efficacy. Thus, a phageome from a cultured fecal donor microbiome may be a more efficient alternative to modulate the gut bacteriome than FMT. Here, we analyzed the dynamic changes of the viromes of mice cecal and human fecal matter inoculated chemostat cultures. Sequencing results showed that the relative abundance of eukaryotic viruses remarkably decreased during continuous cultivation, likely due to the lack of eukaryotic hosts. The corresponding phageome profiles showed dilution rate dependency, a reproducibility between biological replicates, and maintained high diversity of phages although being different from the inoculum phageome. This proof-of-concept study may constitute the first step of developing therapeutic tools to target a broad spectrum of gut-related diseases and thereby replacing FMT with a safer phage-mediated therapy.

## INTRODUCTION

Transplantation of fecal microbiota (FMT) has been successfully applied to treat recurrent *Clostridioides difficile* infections (rCDI) possibly through bacteriophage-mediated (bacterial viruses, in short phages) modulation of the GM landscape [1–4]. The fecal donor material used for FMT is screened for pathogenic bacteria and viruses prior FMT to ensure the safety. However, this process is

34 laborious and may only end up with 3% of the donor candidates passing all safety steps [5], and
35 screening procedures fail, there is risk of transferring disease-causing agents as emphasised by a an
36 incident June 2019 where two patients in the US had severe infections following FMT, of which one
37 patient died [6]. As an alternative to FMT, fecal virome transplantation (FVT, sterile filtrated donor
38 feces) has also shown promising efficacy against CDI and rCDI [2, 7, 8]. An important advantage of FVT
39 over FMT is the elimination of bacterial transfer as a potential threat. However, there is still the risk
40 of transferring disease-causing eukaryotic viruses despite the screening of donor material for known
41 pathogenic viruses as long-term effects of most of the viruses inhabiting the human gastrointestinal
42 tract are not yet studied [9, 10].

43 The interactions between gut bacteria and phages are complex and mutual, hence making the gut
44 virome an important component in health and disease [11, 12]. Microbiome abundances and diversity
45 are predictive of virome richness and diversity [13]. The estimated number of virus-like particles (VLP)
46 remains between $10^9$ and $10^{10}$ VLP per gram of feces [14–17]. The human gut virome is dominated by
47 phages (over 97%) while only about one tenth of those have been annotated until now [18]. The
48 healthy adult gut virome is highly personal and stable over time within each individual [14, 19, 20].
49 Phages belonging to the order *Caudovirales* are together with single stranded DNA phages (ssDNA) of
50 the order *Petitvirales* dominant in the human gut [10–12, 21, 22]. There are several indications that
51 viromes of the dysbiotic and healthy gut microbiota differ [23–25], however the causal links between
52 gut virome dysbiosis and disease is still poorly understood. However, the impact of the phageome on
53 the composition and function of the gut microbiota has been suggested to have important
54 consequences for health and outcome of FMT or FVT treatments [2, 26–29].

55 While phages only infect bacterial and not eukaryotic cells, we aimed to develop methodology to
56 produce active enteric phage communities with minimized amounts of eukaryotic viruses using two
57 different inocula; murine cecal and human fecal microbiota. Of which the chemostat propagated
58 murine gut virome ability to improve gut microbiota balance was evaluated in preclinical studies
59 representing animal models with distinct disease etiologies, CDI [8] and diet-induced obesity [30]. Our
60 recent studies highlighted the importance of dilution rate on the composition of cultured fecal
61 microbiota [31, 32]. The cultivation conditions and substrates were chosen to sustain the highest
62 microbial diversity based on previous knowledge. Dynamics of the chemostat cultures was followed
63 by determination of bacterial and viral composition, growth characteristics and metabolic products.
64 We hypothesized that eukaryotic viruses would be washed out in chemostat culture due to the
65 dilution effect. To our knowledge, the dynamic changes of enteric phages in chemostat cultures have
66 not been described earlier.

67

68 # METHODS

69 **Chemostat inocula**

70 Chemostat cultivations were carried out with two different intestinal inocula of mouse and human
71 origin, respectively. Cecal contents of mice from different vendors were pooled, as previously we have
72 shown that mice from different vendors represents distinctly different gut microbiota profiles (both
73 the bacterial and viral community) [33, 34]. In total 18 C57BL/6N male mice were purchased to harvest
74 intestinal content for downstream applications. The mice were five weeks old at arrival and purchased
75 from three vendors, represented by 6 C57BL/6NTac mice (Taconic, Lille Skensved, Denmark), 6
76 C57BL/6NRj mice (Janvier, Le Genest-Saint Isle, France), and 6 C57BL/6NCrl mice (Charles River,
77 Sulzfeld, Germany) and ear marked at arrival. Animal housing was carried out at Section of
78 Experimental Animal Models, University of Copenhagen, Denmark, under the conditions as described
79 previously [33]. For 13 weeks the mice were fed *ad libitum* low-fat diet (LF, Research Diets D12450J,
80 USA) until termination at 18 weeks old and their body weight were measured every second week. To
81 preserve the viability of the strict anaerobic bacteria, 6 mice from each vendor (in total 18 mice) were
82 sacrificed by cervical dislocation and immediately transferred to a jar containing an anaerobic sachet
83 (cat. no. AN0035A AnaeroGen, Thermo Fisher Scientific) and subsequently to an anaerobic chamber
84 (containing ~93 % $N_2$, ~2 % $H_2$, ~5 % $CO_2$) at room temperature (Model AALC, Coy Laboratory Products,
85 Grass Lake, Michigan, USA) where cecum content of the mice was sampled. Inside the anaerobic
86 chamber, the samples were processed according to vendor (Janvier, Charles River and Taconic);
87 weighted, suspended in an anoxic 1:1 mixture of PBS (NaCl 137 mM, KCl 2.7 mM, Na2HPO4 10 mM,
88 KH2PO4 1.8 mM) and 50% glycerol and homogenized in BagPage® 100 mL filter bags (Interscience,
89 Saint-Nom-la-Bretèche, France) with a laboratory stomacher (Stomacher 80, Seward, UK) at medium
90 speed for 120 seconds. The cecum content from mice from all vendors were mixed, and the pooled
91 cecum content was divided into 6 cryotubes ~ 0.5 g cecum content in each, one for each chemostat
92 run. The samples were frozen and kept at -80°C until use in chemostat experiments. The
93 abovementioned processes are illustrated with a flow-diagram (Supplementary Fig. S1). All
94 procedures regarding the handling of these animals used for donor materiel were carried out in
95 accordance with the Directive 2010/63/EU and the Danish Animal Experimentation Act with the
96 license ID: 2012-15-2934-00256.

97 The human study was approved by Tallinn Medical Research Ethics Committee, Estonia (protocol no.
98 554). Fecal samples from seven healthy donors (age 19-37 years, Caucasian, three male and four

99 female) were diluted five times in dimethyl sulfoxide phosphate saline buffer, pooled in equal volumes
100 and stored frozen at -80°C until use as described previously in Adamberg et al. [35].

101

102 **Growth medium**

103 The base medium was prepared in 0.05 M potassium phosphate buffer containing amino acids,
104 mineral salts and vitamins as described previously [32]. Hemin (5 mg/L), menadione (0.5 mg/L), bile
105 salts (0.5 g/L), NaHCO3 (2.0 g/L), Tween-80 (0.5 g/L), Na-thioglycolate (0.5 g/L) and Cys-HCl (0.5 g/L,
106 freshly made in oxygen reduced water) were added to the base medium. Carbohydrate sources and
107 other components added to the medium for murine cultures were apple pectin (2 g/L, Sigma-Aldrich,
108 USA), chicory inulin HP (1 g/L, Orafti, Belgium), corn core xylan (2 g/L, TCI, Japan), corn starch (5 g/L,
109 Sigma-Aldrich, USA), larch wood arabinogalactan (2 g/L, TCI, Japan) and porcine mucin (4 g/L, Type II,
110 Sigma Aldrich, USA), acetic acid (0.3 g/L, Sigma-Aldrich, USA), tryptone (3 g/L, LABM, UK) and yeast
111 extract (3 g/L, LABM, UK) as described by Macfarlane et al. [36]. Carbohydrate sources for the human
112 fecal matter inoculated cultures were apple pectin (2.5 g/L, Sigma-Aldrich, USA) and porcine mucin
113 (2.5 g/L, Type II, Sigma Aldrich, USA). The carbohydrate sources were sterilized separately and added
114 to the medium before experiments. The medium for mouse cecal matter inoculated cultures
115 contained about three times more carbohydrates than that for human fecal matter inoculated
116 cultures.

117

118 **Cultivation system and culture conditions**

119 The cultivation system described earlier [32] was used for human fecal and mouse cecal matter
120 inoculated cultures. Briefly, the Biobundle cultivation system consisting of fermenter, the ADI 1030
121 bio-controller and cultivation control program "BioXpert" (Applikon, The Netherlands) was used. The
122 fermenter was equipped with sensors for pH, $pO_2$, and temperature control. Variable speed pumps
123 for feeding and outflow were controlled by a chemostat algorithm: D = F/V, where D is the dilution
124 rate (1/h), F is the feeding rate (L/h), and V is the fermenter working volume (L). pH was controlled by
125 adding 1M NaOH according to the pH setpoint. The medium in the feeding bottle and the culture were
126 flushed with sterile-filtered nitrogen gas (99.9%, AS Linde Gas, Estonia) before inoculation and
127 throughout the cultivation to maintain anaerobiosis. The culture volume was kept constant (600 ml
128 for mouse cecal and 300 ml for human fecal matter inoculated cultures). The temperature was kept
129 at 36.6 °C. pH was kept constant at pH=6.4 for mouse cecal and 7.0 for human fecal matter inoculated
130 cultures depending on the physiological pH of the host. The scheme of experiments with mouse cecal
131 matter inoculated culture is depicted in the Fig. 1. Three ml of the pooled mouse cecum matter were
132 inoculated into 600 ml medium to start the experiments. The chemostat algorithm was started 15-20

133 hours after inoculation, which corresponds to the middle of the exponential growth phase of the fecal
134 culture. Three replicates were carried out with human fecal and mouse cecal inocula at two dilution
135 rates, 0.05 1/h ($D_{low}$) and 0.2 1/h ($D_{high}$), except for experiments with mouse cecal inocula at $D_{high}$ where
136 two experiments were performed. The stabilization of five residence times was used in all
137 experiments. On-line and at-line parameters used for experiment control are depicted on the
138 Supplementary Fig. S2.
139
140 **Analytical methods**
141 Samples from the outflow were collected on ice, centrifuged (14,000 g, 5 min, 4 °C) and stored
142 separately as pellets (at -80°C) and supernatants (at -20°C) until further analyses. For chromatographic
143 analyses, culture supernatants were filtered using AmiconR Ultra-10K Centrifugal Filter Devices, cut-
144 off 3 kDa according to the manufacturer's instructions (Millipore, USA). The concentrations of organic
145 acids (succinate, lactate, formate, acetate, propionate, isobutyrate, butyrate, isovalerate and valerate)
146 and ethanol were determined by high-performance liquid chromatography (HPLC, Alliance 2795
147 system, Waters, Milford, MA, USA), using BioRad HPX-87H column (Hercules, CA, USA) with isocratic
148 elution of 0.005 M H2SO4 at a flow rate of 0.5 mL/min and at 35 °C. Refractive index (RI) (model 2414;
149 Waters, USA) and UV (210 nm; model 2487; Waters, USA) detectors. Analytical grade standards were
150 used for quantification of the substances. The detection limit for the method was 0.1 mM.
151 The composition of the gas outflow ($H_2$, $CO_2$, $H_2S$, $CH_4$, and $N_2$) was analyzed using an Agilent 490 Micro
152 GC Biogas Analyzer (Agilent 269 Technologies Ltd., USA) connected to a thermal conductivity detector.
153 The volume of the gas flow was regularly recorded using MilliGascounter (RITTER Apparatebau GMBH
154 & Co, Germany).
155 The Redox potential of the growth medium and culture supernatant was measured by a pH/Redox
156 meter using an InLab®Redox electrode (Mettler Toledo, USA). The biomass dry weight was measured
157 gravimetrically from 10 ml culture by centrifugation (6,000 rpm, 20 min), washing the biomass with
158 distilled water and drying in an oven at 105°C for 20 h.
159
160 **Pre-processing of samples for separation of viruses and bacteria**
161 Culture and inoculum samples were included to investigate microbiome changes over time.
162 Separation of the viruses and bacteria from the culture/inoculum samples generated a pellet and
163 supernatant by centrifugation and 0.45 µm filtering as described previously [33]. The volume of
164 culture/inoculum homogenate was adjusted to 5 mL using SM buffer.
165

166 **Bacterial DNA extraction, sequencing and pre-processing of raw data**

167 Human gut bacteriome data have been previously published [32] but to minimize errors due to using
168 different data processing methods, human gut bacteriome sequences were reanalyzed using the same
169 pipeline as described above for analysis of mice samples. Bead-Beat Micro AX Gravity (mod.1) kit from
170 A&A Biotechnology (Gdynia, Poland) was used to extract bacterial DNA from the culture/fecal pellet
171 by following the instructions of the manufacturer. The final purified DNA was stored at -80ºC and the
172 DNA concentration was determined using Qubit HS Assay Kit (Invitrogen, Carlsbad, California, USA) on
173 the Qubit 4 Fluorometric Quantification device (Invitrogen, Carlsbad, California, USA). The bacterial
174 community composition was determined by NextSeq-based (Illumina) high-throughput sequencing
175 (HTS) of the 16S rRNA gene V3-region, as previously described [24]. Quality-control of reads, de-
176 replicating, purging from chimeric reads and constructing zOTU was conducted with the UNOISE
177 pipeline [37] and taxonomically assigned with Sintax [38]. Taxonomical assignments were obtained
178 using the EZtaxon for 16S rRNA gene database [39]. Code describing this pipeline can be accessed in
179 github.com/jcame/Fastq_2_zOTUtable. The average sequencing depth after quality control
180 (Accession: PRJEB58777, available at ENA) for the fecal 16S rRNA gene amplicons was 60,719 reads
181 (min. 11,961 reads and max. 198,197 reads).

182

183 **Viral RNA/DNA extraction, sequencing and pre-processing of raw data**

184 The sterile filtered culture/fecal supernatant was concentrated using centrifugal filters Centrisart with
185 a filter cut-off at 100 kDA (Sartorius) by centrifugation centrifuged at 1,500 x g at 4ºC
186 (dx.doi.org/10.17504/protocols.io.b2qaqdse). The viral DNA/RNA was extracted from the
187 culture/fecal supernatants using the Viral RNA mini kit (Qiagen) as previously described [33]. Reverse
188 transcription was executed using the SuperScript VILO Master mix by following the instructions of the
189 manufacturer and subsequently cleaned with DNeasy blood and tissue kit (Qiagen) by only following
190 step 3-8 of the manufacturers standard protocol. In brief, the DNA/cDNA samples were mixed with
191 ethanol, bound to the silica filter, washed two times, and eluted with 40 µL elution buffer. Multiple
192 displacement amplification (MDA, to include ssDNA viruses) using GenomiPhi V3 DNA amplification
193 kit (Cytiva) and sequencing library preparation using Nextera XT kit was performed at previously
194 described [33], and sequenced at a commercial facility using the NovaSeq platform (NovoGene). The
195 average sequencing depth of raw reads (Accession: PRJEB58787, available at ENA) for the fecal viral
196 metagenome was 22,701,135 reads (min. 342,022 reads and max. 203,403,294 reads. The raw reads
197 were trimmed from adaptors and the high-quality sequences (>95% quality) using Trimmomatic v0.35
198 [40] with a minimum size of 50 nt were retained for further analysis. High quality reads were de-
199 replicated and checked for the presence of PhiX control using BBMap (bbduk.sh)

200 (https://www.osti.gov/servlets/purl/1241166). Virus-like particle-derived DNA sequences were
201 subjected to within-sample de-novo assembly-only using Spades v3.13.1 [41] and the contigs with a
202 minimum length of 2,200 nt, were retained. Contigs generated from all samples were pooled and de-
203 replicated at 90% identity using BBMap (dedupe.sh). Prediction of viral contigs/genomes was carried
204 out using VirSorter2 [42] ("full" categories | dsDNAphage, ssDNA, RNA, Lavidaviridae, NCLDV |
205 viralquality ≥ 0.66), vibrant [43] (High-quality | Complete), and checkv [44] (High-quality | Complete).
206 Taxonomy was inferred by blasting viral ORF against viral orthologous groups (https://vogdb.org) and
207 the Lowest Common Ancestor (LCA) for every contig was estimated based on a minimum e-value of
208 $10e^{-5}$. Phage-host prediction was determined by blasting (85% identity) CRISPR spacers and tRNAs
209 predicted from >150,000 gut species-level genome bins (SGBs) [45, 46]. Following assembly, quality
210 control, and annotations, reads from all samples were mapped against the viral (high-quality) contigs
211 (vOTUs) using the bowtie2 [47] and a contingency-table of reads per Kbp of contig sequence per
212 million reads sample (RPKM) was generated, here defined as vOTU-table (viral contigs). Code
213 describing this pipeline can be accessed in github.com/jcame/virome_analysis-FOOD. Viral mock
214 communities (phage C2, T7, P35, MS2, Phi6, PhiX174, T4, and PMBT5) were used as positive controls
215 to evaluate if the library preparation and sequencing could detect ss/dsDNA and ss/dsRNA viruses
216 with a titer of ~$10^6$ PFU/mL from both pure phage culture as well as spiked fecal matrices.

217

218 **Bioinformatic analysis of bacterial and viral sequences**

219 Initially the dataset was purged for zOTU's/viral contigs, which were detected in less than 5% of the
220 samples, but the resulting dataset still maintained 99.5% of the total reads. Cumulative sum scaling
221 (CSS) [48] was applied for the analysis of beta-diversity to counteract that a few zOTU/viral contigs
222 represented a large fraction of count values, since CSS have been benchmarked with a high accuracy
223 for the applied metrics [49]. CSS normalization was performed using the R software using the
224 metagenomeSeq package [50]. R version 4.2.2 [51] was used for subsequent analysis and presentation
225 of data. The main packages used were phyloseq [52], vegan [53], deseseq 2 [54], ampvis2 [55], ggpubr,
226 and ggplot2 [56]. A-diversity analysis was based on raw read counts and statistics were based on
227 ANOVA. B-diversity was represented by Bray Curtis dissimilarity metrics and statistics were based on
228 PERMANOVA.

229

230 # RESULTS

231 With the aim of generating viromes depleted of eukaryotic viruses, mouse cecal and human fecal
232 matter were propagated initially as batch cultures and subsequently in chemostat mode at two
233 different dilution rates ($D_{low}$, 0.05 1/h and $D_{high}$, 0.2 1/h) for five residence times. The overall concept

234 for both cultures (i.e dilution rates, temperature, and pH) was the same except for some differences
235 in the media composition. Most importantly, the total carbohydrate concentration was three times
236 higher in the medium for mouse-mimicking conditions compared to that for the human conditions
237 mimicking cultures (15.2 g/L vs 5 g/L, respectively), to resemble the high content of complex
238 carbohydrate in mice chow feed.
239
240 **Wash-out of eukaryotic viruses from chemostat cultures**
241 The relative abundance of eukaryotic viruses decreased already after batch phase and were almost
242 depleted after five residence times in chemostats of both mouse cecal and human fecal matter
243 inoculated cultures (Fig. 2). The relative abundance of eukaryotic viruses after batch phase was
244 0.3±0.2 % and 0.4±0.2 % (average ± standard deviation) in mouse cecal and in human fecal matter
245 inoculated cultures, respectively. During the chemostats relative abundance of eukaryotic viruses
246 declined to 0.006 % and 0.04 % in mice cecal and human fecal matter inoculated cultures at slow
247 dilution rates, respectively. At the same time, the bacterial virome maintained high diversity in the
248 chemostat phase and the number of bacterial viral OTUs remained at least 1000 times higher than
249 these of eukaryotic viral OTUs (Fig. 3 and Supplementary Fig. S3).
250 Both eukaryotic DNA viruses and phages were identified in both inocula (Fig. 3). RNA viruses
251 (*Leviviridae* and *Cystoviridae*) were found only in human feces and their count in mouse cecal matter
252 remained below detection limit of virus particles ($10^6$ VLP/mL). The most abundant taxon of eukaryotic
253 viruses in mouse virome was *Mimiviridae* and the abundances of other identified viral taxa
254 (*Herpesviridae* and *Parvoviridae*) were two magnitudes lower than *Mimiviridae*. Similarly, *Mimiviridae*
255 and *Circoviridae* were the most abundant eukaryotic viruses in human feces. However, their relative
256 abundance from all viruses was below 1%. Of note, nearly half of the vOTUs remained unidentified in
257 both mouse and human inocula.
258
259 **Reproducibility of the chemostat-cultured viromes**
260 Chemostat experiments showed that bacterial and archaeal viruses were persistent to continuous
261 culturing of gut microbiota and showed the dilution rate specific patterns. The diversity of the bacterial
262 virome was significantly related to the dilution rate (Fig. 4). The Shannon index of viromes of mouse
263 cecal matter inoculated cultures remained high even at the end of low dilution rate chemostat while
264 remarkable reductions of diversity were observed at high dilution rate. In cultures inoculated with
265 fecal matter of human origin, no clear associations were seen between the virome diversity and
266 cultivation conditions. However, Shannon indices of bacteriomes of human fecal matter inoculated
267 cultures were higher in chemostats than these in batch cultures (Supplementary Fig. S4). The main

268 archaeal viral taxon was *Bicaudavirus* and its abundance was relatively stable in batch and chemostat
269 modes in both mouse cecal and human fecal matter inoculated cultures (data not shown).
270 When examining overall virome and bacteriome compositional patterns, Fig. 4 shows that inocula and
271 samples of batch, slow and fast chemostat propagation clustered into distinct groups. Viromes of
272 batch samples were closer to these of inoculum samples as there were no outflow but also show
273 persistence of eukaryotic viruses in these conditions. More importantly, our results indicate good
274 reproducibility of chemostat experiments as clearly separated clusters of chemostat samples were
275 observed. Similar distinct clustering was observed also for the bacteriome (see below and
276 Supplementary Fig. S4).
277
278 **The effect of dilution rate on the composition of bacteriomes and corresponding viromes**
279 In mouse cecal matter inoculated batch cultures more than 90% of viral taxa could be identified while
280 in chemostats the number of unidentified viruses increased up to 50% at both dilution rates. In the
281 end of the batch phase, the bacteriome of the mouse cecal matter inoculated culture was dominated
282 by *Bacteroides*, lactobacilli and *Enterobacteriaceae*. Correspondingly, the main taxa of viruses were
283 *Microviridae* and *Siphoviridae* (Fig. 3), which include many viruses related to *Escherichia* and
284 lactobacilli [57, 58]. *Microviridae*, the most abundant taxa in the inoculum decreased significantly
285 already in the batch phase and were mostly washed out for the end of fast chemostat. However, in
286 slow chemostat, *Microviridae* were still present in noticeable amounts by the end of experiment.
287 Other prevalent taxa in the virome at low dilution rate were *Myoviridae* and *Podoviridae*.
288 The most abundant vira in human fecal matter inoculated cultures were also *Microviridae* (more than
289 70%) followed by *Siphoviridae* and *Podoviridae* while the fraction of unidentified viruses remained
290 below 10%. In the end of batch phase the relative abundance of *Microviridae* and other annotated
291 phages decreased while that of unidentified viruses increased several times compared to their
292 proportions in the inocula. At both dilution rates of chemostat cultures, *Microviridae* were mostly
293 washed out and largely replaced by viruses from the family *Myoviridae*, *Podoviridae,* and *Siphoviridae*.
294 *Myoviridae* and *Podoviridae* were especially abundant at high dilution rate.
295 The assembled viral contigs were used to predict bacterial hosts using databases of CRISPR-arrays and
296 tRNA profiles. According to 16S rRNA gene sequence data, the dominant taxa in the mouse inoculum
297 were *Ruminococcaceae*, *Lachnospiraceae* and lactobacilli, which by the end of the batch phase had
298 changed to *Bacteroides*, *Lactobacillus*, *Escherichia* and *Enterobacter* (Fig. 5). In the chemostat cultures
299 with high dilution rates (D = 0.2 1/h), the abundance of these four genera remained high. The
300 abundance of lactobacilli decreased from 23% to 12% while that of *Bacteroides* and enterobacteria
301 remained the most dominant taxa (both more than 20 %) in the end of chemostat propagation. In

302 chemostats with low dilution rate inoculated with mouse cecal matter, *Bifidobacterium*, *Bacteroides*,
303 *Blautia* and an unidentified *Ruminococcaceae* became dominant. At the same time lactobacilli and
304 *Escherichia* were washed out while *Akkermansia*, *Intestinimonas* and an unidentified *Lachnospiraceae*
305 took over their place. Based on the virome host prediction analyses, the prevalence of *Bacteroides*
306 related viruses decreased more than five times at low dilution rate being negligible at the end of
307 chemostat propagation (Supplementary Fig. S4). Higher bacteriome diversity was reflected also in
308 higher virome diversity. There were viruses related to genera *Akkermansia*, *Blautia*, *Enterococcus* and
309 *Lachnoclostridium*, but viruses related to bifidobacteria and *Ruminococcaceae* were not detected
310 (Supplementary Fig. S4).
311 Completely different patterns could be seen in chemostats inoculated with fecal matter of human
312 origin. These were dominated by *Escherichia* and *Enterococcus* in the end of batch phase. It can be
313 explained by the remarkable differences of the composition of human fecal and mouse cecal inocula
314 although the dominant bacterial taxa were comparable. In steady state (end of chemostat), the
315 composition of cultured mouse and human microbiota were more similar. *Bacteroides*,
316 enterobacteria, bifidobacteria and *Clostridium* were abundant in both cultures at high dilution rate
317 while dominance of several *Lachnospiraceae*, *Faecalibacterium* and *Collinsella* was characteristic to
318 human fecal matter inoculated cultures only. On the other hand, *Akkermansia* and *Ruminococcaceae*
319 members were always characteristic of low dilution rate chemostats inoculated with either mouse
320 cecal or human fecal matter. Virome host analysis showed that human fecal matter inoculated
321 cultures contained mainly viruses related to *Bacteroides*, *Faecalibacterium* and *Prevotella* in the end
322 of batch phase (Supplementary Fig. S4). The fast dilution rate promoted propagation of viruses related
323 to *Bacteroides* but also to *Parabacteroides* and *Methanobrevibacter*. The latter was not detected in
324 bacteriome analyses of 16S rRNA gene amplicon sequences.
325
326 **Bacterial metabolites were in accordance with the composition of microbiota**
327 In mouse cecal matter inoculated batch cultures, the major metabolic products were acetate and
328 lactate, comprising about 30 and 24 mol%, respectively, followed by formate, ethanol, succinate and
329 propionate (Fig. 6). Butyrate was almost missing, and propionate represented less than 5 % of total
330 acids. Such metabolite pattern is in accordance with the abundance of lactobacilli, *Bacteroides,*
331 *Enterobacteriaceae* members, and *Bifidobacterium* in mouse cecal matter inoculated batch cultures
332 (Fig. 5).
333 Remarkable differences in product profiles were observed of mouse cecal matter inoculated cultures
334 at two dilution rates, $D_{low}$ = 0.05 1/h and $D_{high}$ = 0.2 1/h (Fig. 6). The highest acetate production (61 ±
335 2 mol-% of total products) was at $D_{low}$, while lactic acid was not detected. Ethanol was produced in

336 comparable amount with butyrate and propionate (all around 10 mol-%). Production of succinate was
337 below 10 mol-% at $D_{low}$ and the amount of formate was marginal (0.1 mol-%) while hydrogen sulfide
338 was mainly detected at $D_{low}$ (1.3 ± 0.1 mmol/gDW) compared to that at $D_{high}$ (0.33 ± 0.03 mmol/gDW).
339 Metabolite data on the human fecal matter inoculated cultures are presented in a recent paper by
340 Adamberg et al [32]. When comparing the cultures of the mouse cecal and human fecal matter
341 inoculated cultures, the overall acid and gas production patterns were similar at high dilution rate
342 ($D_{high}$) but differed at low dilution rate ($D_{low}$). However, propionate production was higher at $D_{low}$ and
343 lactate production was minor at $D_{high}$ in human fecal matter inoculated cultures [32].
344

# 345 DISCUSSION

346 **Reproducibility of the virome propagation**

347 Here we aimed to produce chemostat-propagated gut viromes depleted of eukaryotic viruses. Two
348 different inocula (mouse cecal and human fecal matter) were grown at two different dilution rates,
349 $D_{low}$ = 0.05 and $D_{high}$ = 0.2 1/h. The median relative abundance of contigs of eukaryotic origin decreased
350 from 0.8 % and 0.6 % (mouse cecal and human fecal matter inoculated cultures, respectively) to less
351 than detectable amounts after five residence times in chemostat cultivation. Interestingly, the viromes
352 appeared to be reproducible in replicate runs as both the bacteriomes and the viromes approached
353 equilibrium after five residence times (Supplementary Figs. S3 and S5). It would be expected that
354 extended time of the chemostat process remove more eukaryotic viral particles while maintaining a
355 similar phageome profile. This approach provides a safe and potential effective phage-mediated gut
356 microbiota modulation tool to investigate or treat gut-associated diseases.

357 Very little is known concerning virus profiles of continuous cultures inoculated with fecal or cecal
358 matter. However, the composition of the virome would be expected to be reflected by the bacteriome
359 profile due to their inherent host-phage relationship. Interestingly, the relative abundances of phages
360 did not correspond to their host bacteria in the bacteriome as seen from Figs. 3 and 5. In our study
361 *Siphoviridae* was the dominant viral family in both mouse cecal and human fecal matter inoculated
362 cultures, whilst *Podoviridae* and *Myoviridae* were abundantly present in the human fecal matter
363 inoculated chemostat culture with high dilution rate. *Microviridae*, the most abundant viral family In
364 both inocula was almost washed out in chemostat cultures, excluding slow chemostats started with
365 mouse cecal matter inoculum. High abundance of *Microviridae* in the virome can be explained by
366 method used for sample preparation. Multiple displacement amplification (MDA) has a preference for
367 ssDNA viruses, which might inflate *Microviridae* numbers [59, 60], however, Shah et al. showed
368 recently that using short MDA (half an hour) the data were still quantitative as confirmed by plaque
369 assays of double-stranded DNA (dsDNA) *Escherichia coli* infecting viruses [10].

370

371 **Impact of dilution rate**

372 Dilution rate is a critical factor that determines the composition and metabolism of the chemostat
373 propagated bacteria [36]. This is in line with the human gut transit time (a sort of "dilution rate") being
374 highly correlated to the gut microbiota diversity and composition [61, 62]. Dilution rates 0.2 and 0.05
375 1/h denote the fast degradation of dietary fibers in the cecum and slow grow rate in the colon [31].
376 Microbial metabolism directs the cross feeding between different community members and its
377 changes affects the overall metabolic patterns and composition of the consortium. As an example,
378 *Akkermansia*, a mucus-associated bacterium in the colon [63] was a dominant species in both mouse
379 cecal and human fecal matter inoculated cultures at low dilution rate (0.05 1/h). On the other side the
380 relative abundance of butyric acid producers (species of *Lachnospiraceae*) was higher at high dilution
381 rate (0.2 1/h) [32]. In slow growing mouse cecal matter inoculated cultures higher diversity of the
382 bacteriome was obtained similar to what has also been reported for human fecal matter inoculated
383 chemostats by us and Asnicar et al. [62]. Additionally, high diversity of viromes at $D_{low}$ were shown in
384 this study. Thus, $D_{low}$ in other words appear appropriate to produce diverse microbiomes and
385 phageomes from gut microbiota cultures. In contrast, the growth of *Enterobacteriaceae* and viruses
386 predicted to have *Enterobacteriaceae* as host was remarkably supported by fast dilution ($D_{high}$ = 0.2
387 1/h) in mouse cecal matter inoculated chemostat-fermentations, probably reflecting the high
388 maximum specific growth rate of *Enterobactericeae* [64].

389

390 **Chemostat propagation of active virome for *in vivo* trials**

391 We have shown that chemostat can be used to produce reproducible bacterial consortia from human
392 fecal matter inoculated cultures [32]. In this study we confirmed this phenomenon on mouse cecal
393 matter inoculated cultures and showed also that chemostat can be used to produce reproducible
394 viromes. The chemostat approach showed promising results for propagation of virome with minimal
395 content of eukaryotic viruses [8, 30]. Fecal microbiota transplantation (FMT) allows modification of
396 the intestinal microbiota in medical practice. Although FMT has been shown safe and effective in an
397 immunocompromised CDI cohort [65], for these patients FMT is associated with several threats due
398 to transfer of virulent microbes and viruses [66]. To overcome these potential risks, continuous
399 cultivation of fecal inoculum can be used to diminish the load of eukaryotic viruses by dilution. In the
400 absence of eukaryotic hosts chemostat cultures allow the propagation of bacteria and phage
401 communities. During continuous growth over five volumes the bacterial and viral communities reach
402 stabilized compositions that depend on the cultivation conditions (e.g dilution rate, pH, substrates).

403

404 In conclusion, we showed that chemostat cultivation is a highly promising method to generate mouse
405 cecal and human fecal phageomes with minimal content of eukaryotic viruses. The phage populations
406 can be used in transplantation experiments after removing all bacteria. Using the conditions tested
407 here, the number of eukaryotic viruses can be decreased by more than hundred times of the initial
408 load. This proof-of-concept study may constitute the first step of developing therapeutic tools to
409 target a broad spectrum of gut-related diseases and thereby replacing FMT with a safer phage-
410 mediated therapy.
411

412 # References


413 1. Fujimoto K, Kimura Y, Allegretti JR, Yamamoto M, Zhang Y, Katayama K, et al. Functional
414 Restoration of Bacteriomes and Viromes by Fecal Microbiota Transplantation.
415 *Gastroenterology* 2021; **160**: 2089–2102.
416 2. Ott SJ, Waetzig GH, Rehman A, Moltzau-Anderson J, Bharti R, Grasis JA, et al. Efficacy of
417 Sterile Fecal Filtrate Transfer for Treating Patients With Clostridium difficile Infection.
418 *Gastroenterology* 2017; **152**: 799-811.e7.
419 3. Petrof EO, Gloor GB, Vanner SJ, Weese SJ, Carter D, Daigneault MC, et al. Stool substitute
420 transplant therapy for the eradication of Clostridium difficile infection: 'RePOOPulating' the
421 gut. *Microbiome* 2013; **1**: 1–12.
422 4. Zuo T, Wong SH, Lam K, Lui R, Cheung K, Tang W, et al. Bacteriophage transfer during faecal
423 microbiota transplantation in Clostridium difficile infection is associated with treatment
424 outcome. *Gut* 2018; **67**: 634–643.
425 5. Kassam Z, Dubois N, Ramakrishna B, Ling K, Qazi T, Smith M, et al. Donor Screening for Fecal
426 Microbiota Transplantation. *N Engl J Med* 2019; **381**: 2070–2072.
427 6. DeFilipp Z, Bloom PP, Torres Soto M, Mansour MK, Sater MRA, Huntley MH, et al. Drug-
428 Resistant E. coli Bacteremia Transmitted by Fecal Microbiota Transplant . *N Engl J Med* 2019;
429 **381**: 2043–2050.
430 7. Kao D, Roach B, Walter J, Lobenberg R, Wong K. EFFECT OF LYOPHILIZED STERILE FECAL
431 FILTRATE VS LYOPHILIZED DONOR STOOL ON RECURRENT CLOSTRIDIUM DIFFICILE INFECTION
432 (RCDI): PRELIMINARY RESULTS FROM A RANDOMIZED, DOUBLE-BLIND PILOT STUDY. *J Can*
433 *Assoc Gastroenterol* 2019.
434 8. Rasmussen TS, Forster S, Larsen SB, Von Münchow ASGL, Tranæs KD, Brunse A, et al.
435 Development of safe and effective bacteriophage-mediated therapies against C. difficile
436 infections – a proof-of-concept preclinical study. *bioRxiv* 2023.
437 9. Lim ES, Zhou Y, Zhao G, Bauer IK, Droit L, Ndao IM, et al. Early life dynamics of the human gut

438 virome and bacterial microbiome in infants. *Nat Med* 2015; **21**: 1228–1234.
439 10. Shah SA, Deng L, Thorsen J, Pedersen AG, Dion MB, Castro-Mejía JL, et al. Hundreds of viral
440 families in the healthy infant gut. *Nat Microbiol* 2023.
441 11. Cao Z, Sugimura N, Burgermeister E, Ebert MP, Zuo T, Lan P. The gut virome: A new
442 microbiome component in health and disease. *eBioMedicine* 2022; **81**: 104113.
443 12. Tiamani K, Luo S, Schulz S, Xue J, Costa R, Khan Mirzaei M, et al. The role of virome in the
444 gastrointestinal tract and beyond. *FEMS Microbiol Rev* 2022; **46**: 1–12.
445 13. Corzo-martinez M, García-campos G, Montilla A, Moreno FJ. Tofu whey permeate is an
446 efficient source to enzymatically produce prebiotic fructooligosaccharides and novel
447 fructosylated # -galactosides. *J Agric Food Chem* 2016.
448 14. Shkoporov AN, Clooney AG, Sutton TDS, Ryan FJ, Daly KM, Nolan JA, et al. The Human Gut
449 Virome Is Highly Diverse, Stable, and Individual Specific. *Cell Host Microbe* 2019; **26**: 527-
450 541.e5.
451 15. Shkoporov AN, Hill C. Bacteriophages of the Human Gut: The "Known Unknown" of the
452 Microbiome. *Cell Host Microbe* 2019; **25**: 195–209.
453 16. Lepage P, Colombet J, Marteau P, Sime-Ngando T, Doré J, Leclerc M. Dysbiosis in
454 inflammatory bowel disease: A role for bacteriophages? *Gut* 2008; **57**: 424–425.
455 17. Hoyles L, McCartney AL, Neve H, Gibson GR, Sanderson JD, Heller KJ, et al. Characterization of
456 virus-like particles associated with the human faecal and caecal microbiota. *Res Microbiol*
457 2014; **165**: 803–812.
458 18. Gregory AC, Zablocki O, Zayed AA, Howell A, Bolduc B, Sullivan MB. The Gut Virome Database
459 Reveals Age-Dependent Patterns of Virome Diversity in the Human Gut. *Cell Host Microbe*
460 2020; **28**: 724-740.e8.
461 19. Manrique P, Bolduc B, Walk ST, Van Oost J Der, De Vos WM, Young MJ. Healthy human gut
462 phageome. *Proc Natl Acad Sci U S A* 2016; **113**: 10400–10405.
463 20. Minot S, Sinha R, Chen J, Li H, Keilbaugh SA, Wu GD, et al. The human gut virome: Inter-
464 individual variation and dynamic response to diet. *Genome Res* 2011; **21**: 1616–1625.
465 21. Spencer L, Olawuni B, Singh P. Gut Virome: Role and Distribution in Health and
466 Gastrointestinal Diseases. *Front Cell Infect Microbiol* 2022; **12**: 1–11.
467 22. Broecker F, Russo G, Klumpp J, Moelling K. Stable core virome despite variable microbiome
468 after fecal transfer. *Gut Microbes* 2017; **8**: 214–220.
469 23. Norman JM, Handley SA, Baldridge MT, Droit L, Liu CY, Keller BC, et al. Disease-specific
470 alterations in the enteric virome in inflammatory bowel disease. *Cell* 2015; **160**: 447–460.
471 24. Tao Z. Unveiling the gut virome in human health and diseases. *Int J Clin Virol* 2018; **2**: 001–

472 003.
473 25. Clooney AG, Sutton TDS, Shkoporov AN, Holohan RK, Daly KM, O'Regan O, et al. Whole-
474 Virome Analysis Sheds Light on Viral Dark Matter in Inflammatory Bowel Disease. *Cell Host*
475 *Microbe* 2019; **26**: 764-778.e5.
476 26. Brunse A, Deng L, Pan X, Hui Y, Castro-Mejía JL, Kot W, et al. Fecal filtrate transplantation
477 protects against necrotizing enterocolitis. *ISME J* 2022; **16**: 686–694.
478 27. Beller L, Deboutte W, Vieira-Silva S, Falony G, Tito RY, Rymenans L, et al. The virota and its
479 transkingdom interactions in the healthy infant gut. *Proc Natl Acad Sci U S A* 2022; **119**.
480 28. Rasmussen TS, Mentzel CMJ, Kot W, Castro-Mejía JL, Zuffa S, Swann JR, et al. Faecal virome
481 transplantation decreases symptoms of type 2 diabetes and obesity in a murine model. *Gut*
482 2020; **69**: 2122–2130.
483 29. Rasmussen TS, Koefoed AK, Jakobsen RR, Deng L, Castro-Mejia JL, Brunse A, et al.
484 Bacteriophage-mediated manipulation of the gut microbiome-promises and presents
485 limitations. *FEMS Microbiol Rev* 2020; **44**: 507–521.
486 30. Mao X, Larsen SB, Zachariassen LSF, Brunse A, Adamberg S, Castro Mejia JL, et al. A
487 reproducible enteric phage community improves blood glucose regulation in an obesity
488 mouse model. *bioRxiv* 2023.
489 31. Adamberg K, Adamberg S. Selection of fast and slow growing bacteria from fecal microbiota
490 using continuous culture with changing dilution rate. *Microb Ecol Health Dis* 2018; **29**:
491 1549922.
492 32. Adamberg K, Raba G, Adamberg S. Use of Changestat for Growth Rate Studies of Gut
493 Microbiota. *Front Bioeng Biotechnol* 2020; **8**: 1–12.
494 33. Rasmussen TS, de Vries L, Kot W, Hansen LH, Castro-Mejía JL, Vogensen FK, et al. Mouse
495 vendor influence on the bacterial and viral gut composition exceeds the effect of diet. *Viruses*
496 2019; **11**.
497 34. Rasmussen TS, Jakobsen RR, Castro-Mejía JL, Kot W, Thomsen AR, Vogensen FK, et al. Inter-
498 vendor variance of enteric eukaryotic DNA viruses in specific pathogen free C57BL/6N mice.
499 *Res Vet Sci* 2021; **136**: 1–5.
500 35. Adamberg K, Tomson K, Talve T, Pudova K, Puurand M, Visnapuu T, et al. Levan enhances
501 associated growth of Bacteroides, Escherichia, Streptococcus and Faecalibacterium in fecal
502 microbiota. *PLoS One* 2015.
503 36. Macfarlane GT, Macfarlane S, Gibson GR. Validation of a Three-Stage Compound Continuous
504 Culture System for Investigating the Effect of Retention Time on the Ecology and Metabolism
505 of Bacteria in the Human Colon. *Microb Ecol* 1998; **44**: 180–187.

506 37. Edgar RC. Updating the 97% identity threshold for 16S ribosomal RNA OTUs. *Bioinformatics*
507 2018; **34**: 2371–2375.
508 38. Edgar R. SINTAX: a simple non-Bayesian taxonomy classifier for 16S and ITS sequences.
509 *bioRxiv* 2016; 074161.
510 39. Kim OS, Cho YJ, Lee K, Yoon SH, Kim M, Na H, et al. Introducing EzTaxon-e: A prokaryotic 16s
511 rRNA gene sequence database with phylotypes that represent uncultured species. *Int J Syst*
512 *Evol Microbiol* 2012; **62**: 716–721.
513 40. Bolger AM, Lohse M, Usadel B. Trimmomatic: A flexible trimmer for Illumina sequence data.
514 *Bioinformatics* 2014; **30**: 2114–2120.
515 41. Bankevich A, Nurk S, Antipov D, Gurevich AA, Dvorkin M, Kulikov AS, et al. SPAdes: A new
516 genome assembly algorithm and its applications to single-cell sequencing. *J Comput Biol*
517 2012; **19**: 455–477.
518 42. Guo J, Bolduc B, Zayed AA, Varsani A, Dominguez-Huerta G, Delmont TO, et al. VirSorter2: a
519 multi-classifier, expert-guided approach to detect diverse DNA and RNA viruses. *Microbiome*
520 2021; **9**: 1–13.
521 43. Kieft K, Zhou Z, Anantharaman K. VIBRANT: Automated recovery, annotation and curation of
522 microbial viruses, and evaluation of viral community function from genomic sequences.
523 *Microbiome* 2020; **8**: 1–23.
524 44. Nayfach S, Camargo AP, Schulz F, Eloe-Fadrosh E, Roux S, Kyrpides NC. CheckV assesses the
525 quality and completeness of metagenome-assembled viral genomes. *Nat Biotechnol* 2021;
526 **39**: 578–585.
527 45. Pasolli E, Asnicar F, Manara S, Zolfo M, Karcher N, Armanini F, et al. Extensive Unexplored
528 Human Microbiome Diversity Revealed by Over 150,000 Genomes from Metagenomes
529 Spanning Age, Geography, and Lifestyle. *Cell* 2019; **176**: 649-662.e20.
530 46. Castro-Mejía JL, Khakimov B, Aru V, Lind M V., Garne E, Paulová P, et al. Gut Microbiome and
531 Its Cofactors Are Linked to Lipoprotein Distribution Profiles. *Microorganisms* 2022; **10**: 1–15.
532 47. Langmead B, Salzberg SL. Fast gapped-read alignment with Bowtie 2. *Nat Methods* 2012; **9**:
533 357–359.
534 48. Paulson JN, Colin Stine O, Bravo HC, Pop M. Differential abundance analysis for microbial
535 marker-gene surveys. *Nat Methods* 2013; **10**: 1200–1202.
536 49. Weiss S, Xu ZZ, Peddada S, Amir A, Bittinger K, Gonzalez A, et al. Normalization and microbial
537 differential abundance strategies depend upon data characteristics. *Microbiome* 2017; **5**: 1–
538 18.
539 50. Paulson J. metagenomeSeq: Statistical analysis for sparse high-throughput sequencing.

540 *BioconductorJp* 2014; 1–20.
541 51. Team RC. R Core TeamR: A language and environment for statistical computing. R Foundation
542 for Statistical Computing, Vienna, Austria. 2018.
543 52. McMurdie PJ, Holmes S. Phyloseq: An R Package for Reproducible Interactive Analysis and
544 Graphics of Microbiome Census Data. *PLoS One* 2013; **8**.
545 53. Philip D. Computer program review VEGAN , a package of R functions for community ecology.
546 *J Veg Sci* 2003; **14**: 927–930.
547 54. Love MI, Huber W, Anders S. Moderated estimation of fold change and dispersion for RNA-
548 seq data with DESeq2. *Genome Biol* 2014; **15**: 1–21.
549 55. Andersen KS, Kirkegaard RH, Karst SM, Albertsen M. ampvis2: An R package to analyse and
550 visualise 16S rRNA amplicon data. *bioRxiv* 2018; 10–11.
551 56. Wickham H. Ggplot2. *Wiley Interdiscip Rev Comput Stat* 2011; **3**: 180–185.
552 57. Niu YD, McAllister TA, Nash JHE, Kropinski AM, Stanford K. Four Escherichia coli O157:H7
553 phages: A new bacteriophage genus and taxonomic classification of T1-like phages. *PLoS One*
554 2014; **9**.
555 58. Marcó MB, Garneau JE, Tremblay D, Quiberoni A, Moineau S. Characterization of two virulent
556 phages of Lactobacillus plantarum. *Appl Environ Microbiol* 2012; **78**: 8719–8734.
557 59. d'Humières C, Touchon M, Dion S, Cury J, Ghozlane A, Garcia-Garcera M, et al. A simple,
558 reproducible and cost-effective procedure to analyse gut phageome: from phage isolation to
559 bioinformatic approach. *Sci Rep* 2019; **9**: 25–28.
560 60. Yilmaz S, Allgaier M, Hugenholtz P. Multiple displacement amplification compromises
561 quantitative analysis of metagenomes. *Nat Methods* 2010; **7**: 943–944.
562 61. Müller M, Hermes GDA, Canfora EE, Smidt H, Masclee AAM, Zoetendal EXG, et al. Distal
563 colonic transit is linked to gut microbiota diversity and microbial fermentation in humans
564 with slow colonic transit. *Am J Physiol - Gastrointest Liver Physiol* 2020; **318**: G361–G369.
565 62. Asnicar F, Leeming ER, Dimidi E, Mazidi M, Franks PW, Al Khatib H, et al. Blue poo: Impact of
566 gut transit time on the gut microbiome using a novel marker. *Gut* 2021; **70**: 1665–1674.
567 63. de Vos WM. Microbe profile: Akkermansia muciniphila: A conserved intestinal symbiont that
568 acts as the gatekeeper of our mucosa. *Microbiol (United Kingdom)* 2017; **163**: 646–648.
569 64. Schaechter M, Maaloe O, Kjeldgaard N. Dependency on medium and temperature of cell size
570 and chemical composition …. *Microbiology* 1958.
571 65. Suchman K, Luo Y, Grinspan A. Fecal Microbiota Transplant for Clostridioides Difficile
572 Infection Is Safe and Efficacious in an Immunocompromised Cohort. *Dig Dis Sci* 2022; **67**:
573 4866–4873.

574 66. Shogbesan O, Poudel DR, Victor S, Jehangir A, Fadahunsi O, Shogbesan G, et al. A Systematic
575 Review of the Efficacy and Safety of Fecal Microbiota Transplant for Clostridium difficile
576 Infection in Immunocompromised Patients. *Can J Gastroenterol Hepatol* 2018; **2018**.
577
578

# Figures

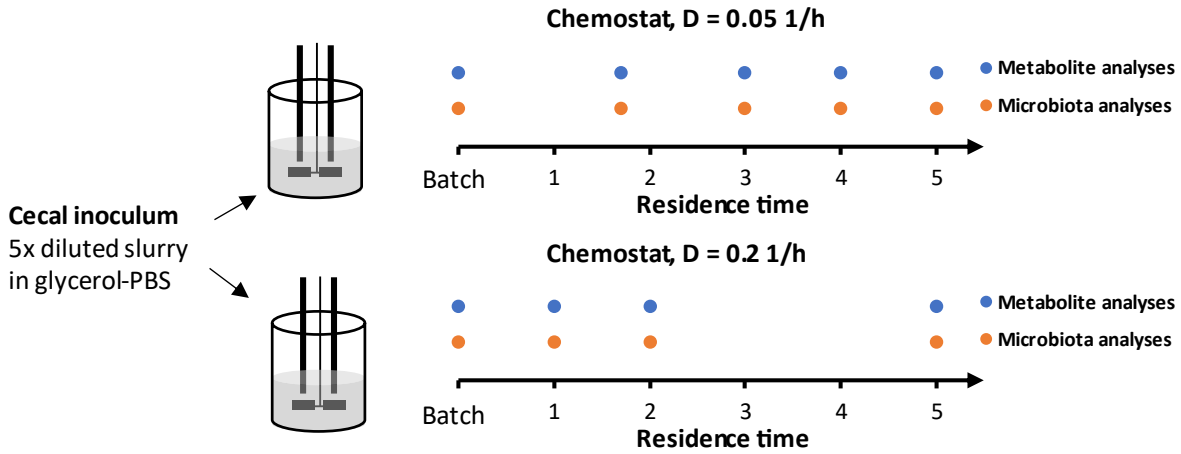


Fig. 1. The experimental setup of chemostat cultivations of mice cecal culture. At start one percent of five times diluted cecal content was inoculated into a bioreactor followed by batch growth 23 h. The chemostat culture was then run up to 5 residential times. Colored dots indicate the sampling points for metabolite and microbiota (16S rRNA gene amplicon and virome sequencing) analyses. Similar setup was used for human fecal cultures [32].

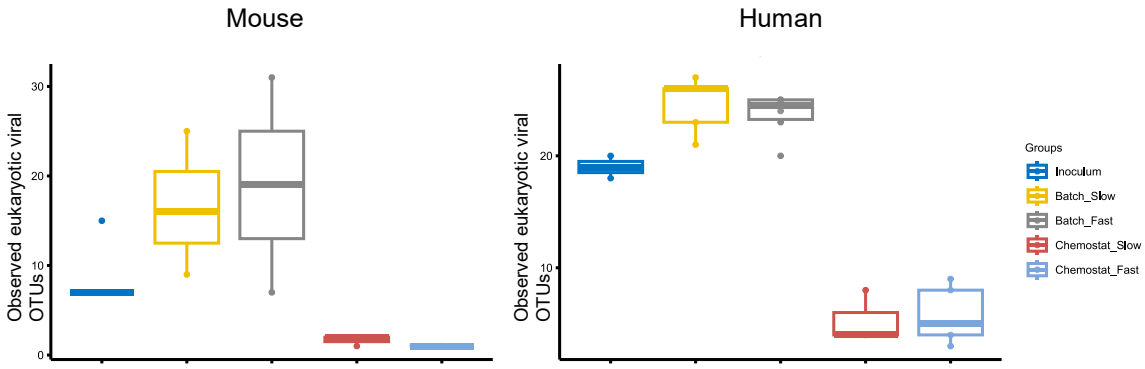


Fig. 2. Chemostat propagation of cecal/ fecal inocula leads to depletion of eukaryotic viruses shown as the number or observed eukaryotic viral operational taxonomic units (vOTUs). Batch_Slow and Batch_Fast designate the batch cultures prior the chemostat mode of low and fast dilution rates, respectively.

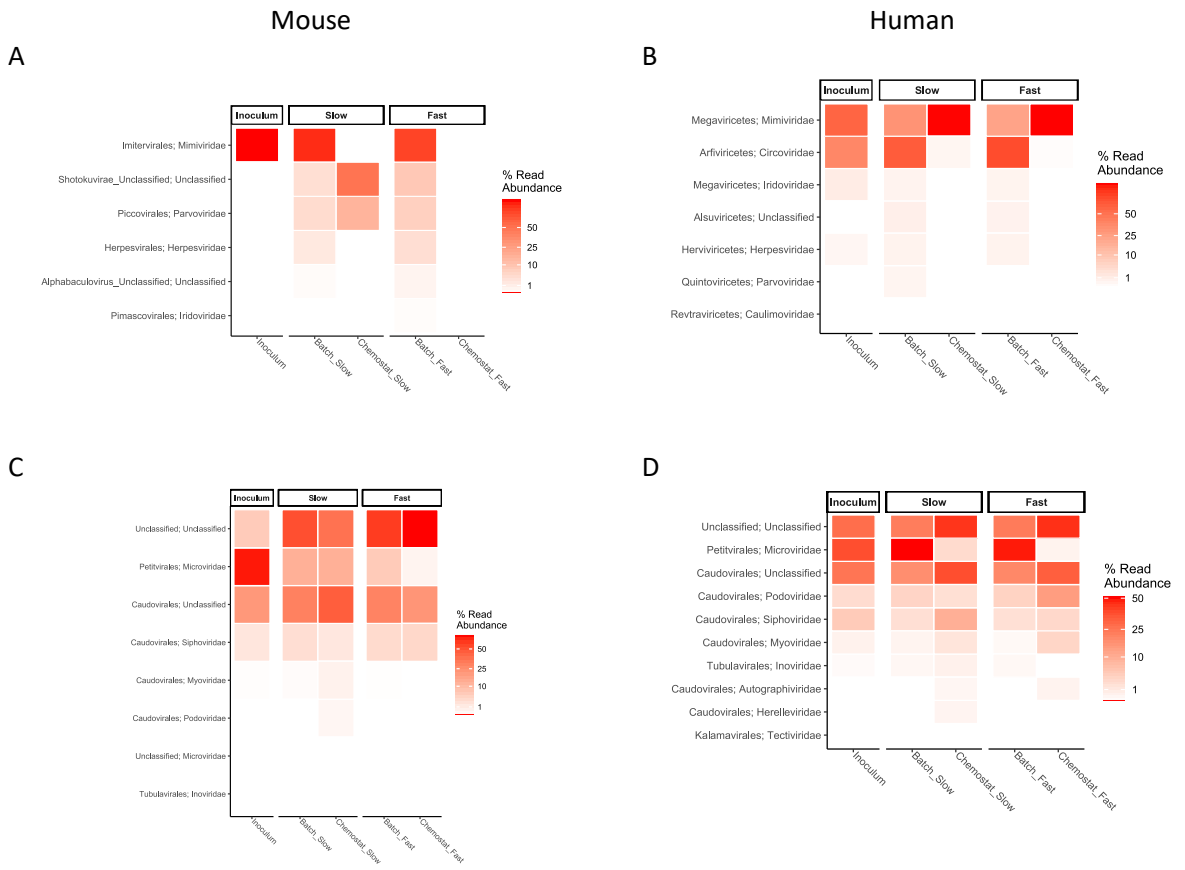


Fig. 3. Diversity of prokaryotic viruses during chemostat propagation of mouse cecal/ human fecal matter inoculated cultures. Depletion of eukaryotic viral families and enrichment of bacterial viral families from batch to stabilized chemostat cultures (A and C – mouse cecal matter inoculated cultures, B and D – human fecal matter inoculated cultures) presented as heatmaps. Color intensity indicates the relative abundance of eukaryotic (A, B) or prokaryotic (C, D) viral contigs from total eukaryotic or prokaryotic viral contigs, respectively. 'Slow' and 'Fast' indicate the dilution rates used in the chemostat ($D_{low}$ 0.05 and $D_{high}$ 0.2 1/h, respectively). Batch_Slow and Batch_Fast designate the batch cultures prior the corresponding chemostat modes of low and fast dilution rates, respectively.

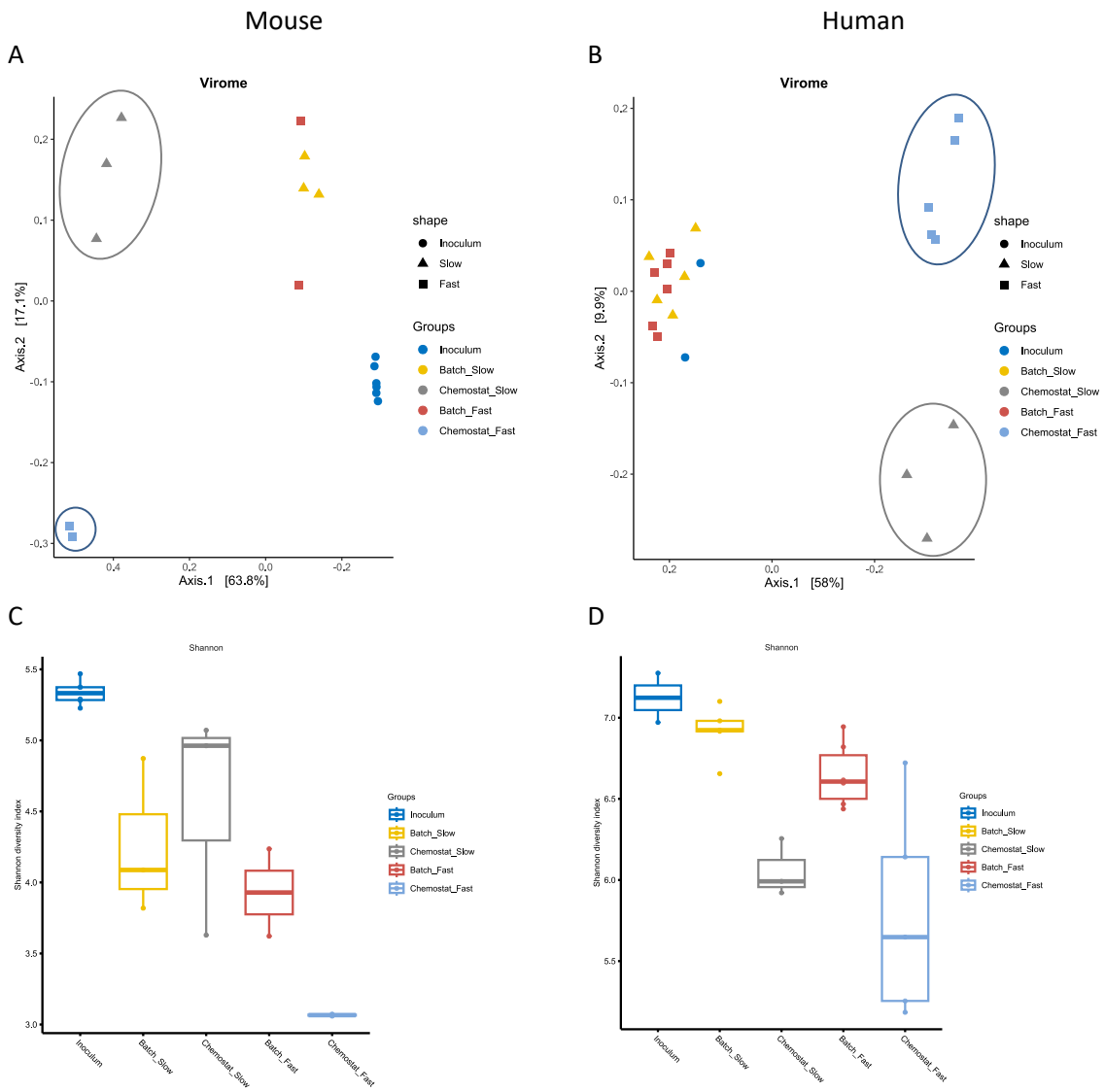


603

604 Fig. 4. Chemostat propagation of fecal inocula at different dilution rates leads to viromes with
605 reproducible composition shown by beta diversity (A, B) and diverse viral community shown by
606 Shannon index (C, D). Samples from inoculum, batch and chemostat cultures of mouse cecal (A, C) and
607 human fecal (B, D) matter inoculated cultures are shown. 'Slow' and 'fast' in the column names
608 indicate the dilution rate used in the chemostat ($D_{low}$ 0.05 and $D_{high}$ 0.2 1/h, respectively). Batch_Slow
609 and Batch_Fast designate the batch cultures prior the corresponding chemostat modes of low and fast
610 dilution rates, respectively. Beta diversity and Shannon indices of bacteriomes are shown on the
611 Supplementary Fig. S4.

612

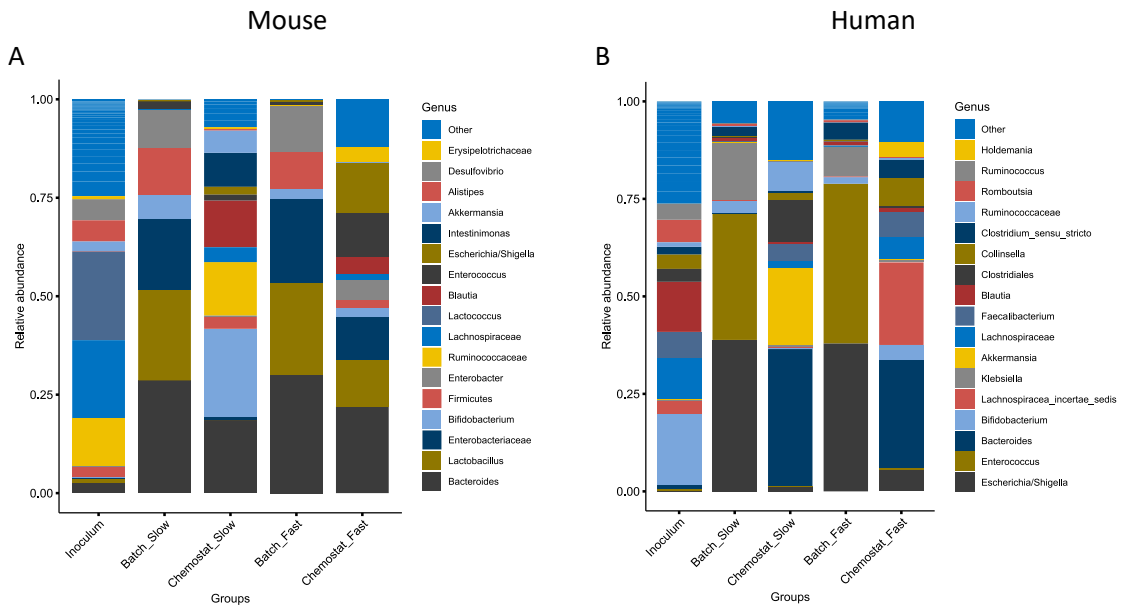


Fig. 5. Bacteriome composition of mice cecal (A) and human fecal matter inoculated cultures (B) after batch and chemostat propagation. 'Slow' and 'fast' in the column names indicate the dilution rate used in the chemostat ($D_{low}$ 0.05 and $D_{high}$ 0.2 1/h, respectively). Batch_Slow and Batch_Fast designate the batch cultures prior the corresponding chemostat modes of low and fast dilution rates, respectively.

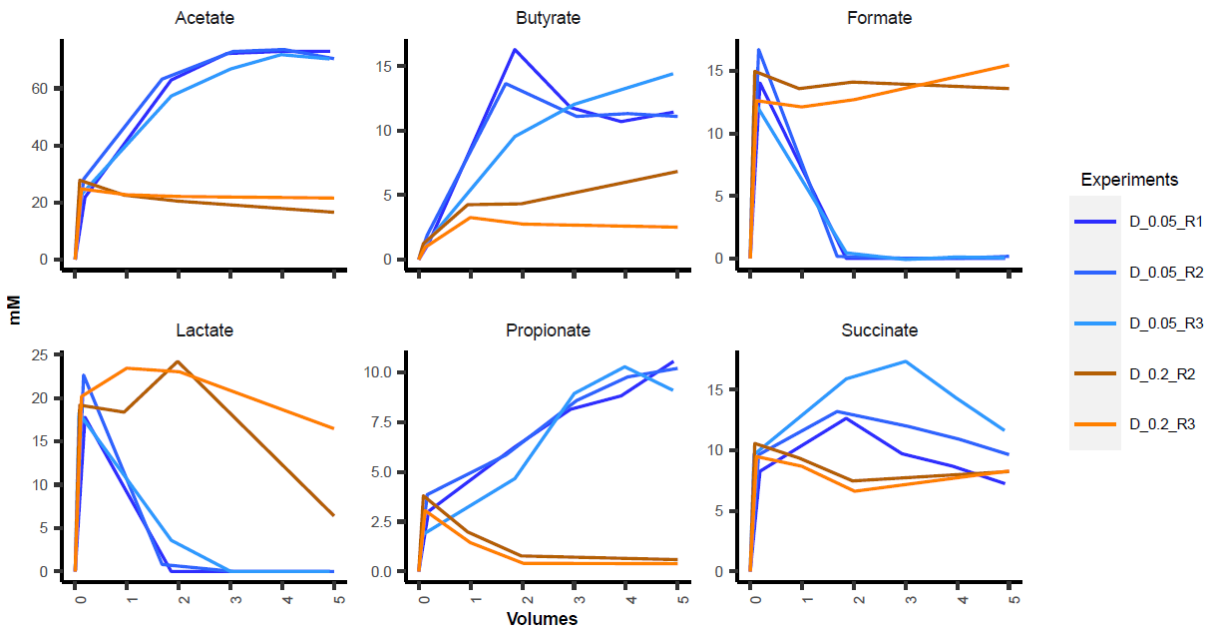


Fig. 6. Reproducibility of metabolite dynamics of chemostat propagated mouse cecal cultures at two dilution rates. Metabolite concentrations are shown in millimoles in relation to residence time ('Volumes' on x-scale). Low dilution rate (D = 0.05 1/h) is indicated with blue lines and high dilution rate (D = 0.2 1/h) with brown-orange lines. R indicates the number of the replicate.